ELSEVIER

Journal of Hazardous Materials B87 (2001) 199–212

Journal of Hazardous Materials

www.elsevier.com/locate/jhazmat

# Non-passivating polymeric structures in electrochemical conversion of phenol in the presence of NaCl

M.H. Zareie [a], Bahadır K. Körbahti [b], Abdurrahman Tanyolaç [b,*]

[a] *School of Physics, University of Sydney, 2001 Sydney, NSW, Australia*
[b] *Chemical Engineering Department, Faculty of Engineering, Hacettepe University, Beytepe, 06532 Ankara, Turkey*

Received 21 November 2000; received in revised form 3 May 2001; accepted 24 May 2001

**Abstract**

The formation of non-passivating polymeric structures was investigated during electrochemical conversion of phenol using carbon electrodes and NaCl as electrolyte. The influence of initial phenol concentration, current density and reaction temperature on phenol conversion and polymer morphology was studied by FTIR and STM, while the fate of intermediate compounds was analyzed by GC/MS. Unlike previous work, non-passivating solid polymer was produced at high voltage and current density values in the presence of NaCl. The most orderly polymer formed at 912 mg $l^{-1}$ initial phenol concentration, current density 32.9 mA $cm^{-2}$, NaCl concentration 120 g $l^{-1}$ and temperature 25°C. Higher operational parameters yielded disorderly formed aggregates of the polymer in decreasing surface density on STM images. Along with the polymer, only toxic mono-, di- and tri-chlorophenols were formed as intermediate compounds during the electrochemical conversion, which eventually were polymerized and/or oxidized to final products. FTIR analysis and enlarged STM image implied the repeating phenol units in the polymer structure. The results may lead to appropriate techniques for the removal of phenol from wastewater in the form of a solid polymer.


*Keywords:* Phenol; Electrochemical conversion; Polymer; Scanning tunneling microscopy (STM); NaCl

## 1. Introduction

The removal of phenolic compounds from wastewater is of environmental importance due to high oxygen demand and chemical toxicity. Phenols are frequently found in the

* Corresponding author. Tel.: +90-312-297-7404; fax: +90-312-299-2124.
*E-mail address:* tanyolac@hacettepe.edu.tr (A. Tanyolaç).

0304-3894/01/$ – see front matter 
PII: S0304-3894(01)00278-3

wastewater of most processes involving aromatic organic chemicals. Some of the larger and more common sources are; paper and pulp mills, petrochemical refineries, some plastic and glue manufacturers and coke plants. Under appropriate circumstances, phenols can be economically recovered from water at concentrations above 2000–4000 mg $l^{-1}$. Below this level, destruction must be used via biological, physico-chemical and chemical processes [1].

Of the various chemical processes, electrochemical oxidation for destruction of phenolic wastes have been investigated [2–8] and pilot studies have been carried out but not used commercially due to a low phenol reaction rate or low efficiency [7,9]. One strong reason for the low reaction rate found with electrochemical oxidation of some organic compounds is electrode fouling. Phenol is well known for its ability to foul electrodes and the tarry deposit forming on electrodes during phenol oxidation is attributed to phenolic polymerization products. The oxidation of phenolic compounds at solid electrodes produces phenoxy radicals, which are responsible for coupling to form a passivating polymeric film on the electrodes [6]. Using phenol and substituted phenols for anodic oxidation in alkaline media, either thin films (1000 Å) [10] or relatively thick coatings (>10 μm) [11,12] have been obtained depending on the reaction conditions. Various strategies have been developed to address these surface fouling problems including the use of electrochemical pre-treatment [13,14], laser activation [15], chemical or electrochemical treatment [5,8] and reducing the concentration and lifetime of phenoxy radicals [8,16,17]. The formation rate of tar depends on radical concentration, which can be limited by decreasing the concentration of phenol and minimizing the current density. Radical lifetime can be decreased by decreasing reaction pH because the phenol oxidation potential decreases with pH while the phenoxy radical oxidation potential remains unchanged [8].

Despite the significance of the phenolic polymer deposition on electrodes, only a limited number of investigators have attempted to characterize the structure of the film. Lapuente et al. [18] employed FTIR–ATR to investigate polyphenol films formed on platinum surfaces by electrochemical oxidation of phenol in aqueous carbonate solutions with and without $Na_2S$. Using IR spectroscopy and ex situ X-ray photoelectron spectroscopy (XPS) Dubois and coworkers [19–21] have determined chemical and physical properties of polymeric films created in hydroalcoholic solutions. Gattrell and Kirk [6,8,22] have used FTIR spectroscopy to analyze samples of the passivated film produced on a platinum electrode during phenol electrolysis in sulfuric acid medium. A Raman spectroscopic investigation of the phenol electropolymerization on silver electrodes was performed in methanol and water mixtures in the presence and absence of amines [23]. Richard and Gewirth studied the behavior of phenoxide on Au(1 1 1) during electrooxidation in alkaline solutions using FTIR, STM and AFM [24]. Some investigators have obtained scanning electron micrographs (SEMs) of the deposited films [18] but so far, there are very few studies on imaging the polyphenol films with STM [24,25].

The advent of scanning tunneling microscopy (STM) [26] provides a powerful high resolution imaging technique, which can be used to study these films. The possibility of operating an STM under atmospheric conditions with air-dried samples helps maintain the surface structure, which have, in principle, sufficient electrical conductivity. Recently, it has been shown that thin polymer films, of polyethylene [27,28], poly(1-butene) [29], polybutadiene [30], poly(MMA/BMA) [31] can be investigated by STM.

In this work, we investigated the conditions for the formation of the non-passivating polymeric structures during the anodic electrochemical conversion of phenol using carbon electrodes in the presence of NaCl. In literature, there has not been any work reporting the formation of the non-passivating solid polymer during electrochemical conversion of phenol carried out with NaCl electrolyte. In batch runs, the effects of current density, initial phenol concentration and process temperature on phenol conversion and polymer formation were elucidated. The fate of toxic intermediate products was monitored with sequential GC/MS analysis and the polymer structure was discussed in the view of experimental conditions, STM images, FTIR analysis and literature experience.

## 2. Experimental

### *2.1. Materials*

Phenol (Merck) and NaCl (Merck) were used as received. Double distilled and deionized water was used in all experiments. The solvents chloroform and methanol were obtained from Merck as extra pure reagents, unless otherwise stated.

### *2.2. Methods*

#### *2.2.1. Experimental set-up and procedure*

The polymer was produced during the electrochemical oxidation of phenol in the NaCl electrolyte solution. All runs were carried out batch-wise in a mixed electrochemical reactor as sketched in Fig. 1. The 2 l cylindrical reactor was made of Pyrex glass with a cooling/heating jacket, having three pairs of carbon electrodes, for anode and cathode, placed 8 cm apart on a Plexiglas reactor cover. A glass stirrer with a single 4.5 cm paddle

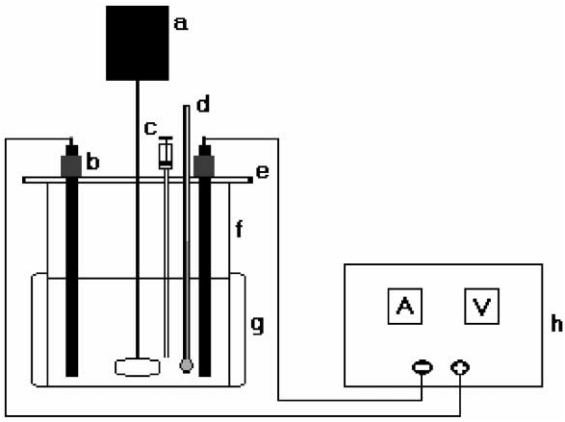


Fig. 1. The schematic view of electrochemical batch reactor: (a) driving motor and glass stirrer; (b) electrodes; (c) sampling injector; (d) thermometer; (e) Plexiglas reactor cover; (f) reactor; (g) heating/cooling jacket; (h) dc power source.

agitator was used to homogenize the system. The reaction temperature was controlled by a temperature water bath (model G-86, New Brunswick). Current was applied by a constant voltage or current controlled dc power source (Netes NPS-181OD). A typical phenol electrochemical oxidation/polymerization procedure was as follows; 1 l of synthetic phenolic wastewater was prepared by dissolving appropriate amounts of phenol and NaCl, the electrolyte, in distilled water. The reaction started with the application of specified current density and the solution was mixed at a constant 450 rpm. At half-hour intervals, 10 ml of samples were drawn from the system for phenol analysis. The reaction was ceased when either 99% of initial phenol was converted or 8 h elapsed, whichever came first, by turning-off the power. Then non-sticky solid polymer particles with the particle diameter distribution; 0–250 μm 4.2%, 250–500 μm 69.9%, 500–750 μm 18.2% and 750–1000 μm 7.7%, was filtered from the solution. The solid product was washed several times successively with distilled water to remove impurities. Then, as described previously [32], the polymer was dissolved in pure chloroform, filtered and precipitated in a large amount of pure methanol. The polymer was washed with distilled water again and dried in a vacuum tube at 30°C until constant weight was reached.

*2.2.2. The reaction conditions*

The effects of initial phenol concentration, reaction temperature and applied current density on the polymer samples were investigated. The experiments for initial phenol concentration effects were carried out in 98–4698 mg $l^{-1}$ phenol concentration at 25°C with 120 g $l^{-1}$ electrolyte concentration and 32.9 mA $cm^{-2}$ current density. The influence of reaction temperature was studied for the temperatures 25–40°C at 3500 mg $l^{-1}$ and 120 g $l^{-1}$ initial phenol and electrolyte concentrations, respectively. For current density experiments, applied current density was changed in the range 9.6–63.9 mA $cm^{-2}$ at 25°C with 3500 mg $l^{-1}$ and 200 g $l^{-1}$ initial phenol and electrolyte concentrations, respectively.

*2.2.3. Analysis*

STM images of the polymer samples produced under different reaction conditions were obtained. Then, the FTIR spectrum of the polymer produced at 25°C with 120 g $l^{-1}$ and 2246 mg $l^{-1}$ electrolyte and initial phenol concentrations, respectively, under 32.9 mA $cm^{-2}$ current density, which were the reasonable conditions for a long chain polymer formation, were analyzed.

The STM used in this work was constructed in our laboratory [33]. In order to obtain STM images of the polymer and its film formation, the purified polymer was dissolved in AR grade acetone at 2 mg $ml^{-1}$ concentration and 10 μl of the liquid sample was deposited onto freshly cleaved highly oriented pyrolitic graphite (HOPG) surfaces. HOPG was selected as the substrate because it is clean, inert, conductive, and free of defect over a large area. Moreover, since the surface of HOPG is known, the STM images obtained cannot be confused with that of the polymer. After drying at room temperature, the sample of the polymer product was directly imaged in air. For all images, the STM was operated in the constant current mode at ambient temperature (21°C) and atmospheric pressure. Individual samples were imaged using a range of operating parameters, but typical imaging conditions were 2 V sample bias and a tunneling current of a 20 pA. The typical tip voltage and current values were selected as 800 mV and 1 nA. Cut tips of Pt/Ir (80:20) wire (0.5 mm in diameter, Digital Instruments,

Santa Barbara, CA) were used. Prior to use, the tips were washed with AR grade acetone and dried in air.

For FTIR analysis, 2.5 mg purified polymer was mixed completely with IR grade 200 mg KBr and homogenized in a mortar. About 60 mg of this sample was pressed in the form of a tablet, and the spectrum was recorded using a FTIR (Unicam Mattson 1000).

The change in phenol concentration of the reaction medium was determined by means of a Cecil 1100 HPLC system. This system was equipped with a variable wavelength monitor (CE 11220) operating at 254 nm and a Cecil HPLC pump system (CE 1100). Chromatograms were obtained using a Hichrom-S5OS1 column (Chromosorb). Only one mobile phase, running at ambient temperature, was eluted and 20 ml sample was injected. Methanol/water (40/60 (v/v)) was used as the mobile phase and the flow rate was adjusted to 1.0 ml $min^{-1}$ under 28 MPa pressure. Before the analysis, the mobile phase was filtered and sonicated in order to remove dissolved gases.

For GC/MS analysis of intermediate electrooxidation products, 5 ml liquid sample was taken from the reactor at appropriate time intervals. The pH of the sample was adjusted to 3 with $HNO_3$ and aqueous phase was saturated with NaCl. Then the sample was extracted for 20 min with 5 ml of diethyl ether, organic phase was separated in a separation funnel and 1 ml of ether phase was injected into GC/MS system (5972 MSD attached 5890 HP GC). A DB-1 capillary column was used for the separation and oven temperature was programmed as constant 50°C for 1 min, then increased to 250°C with 20°C $min^{-1}$ rate and finally 10 min at 250°C. Automatic injection system was kept at 250–280°C while mass detector temperature was held at 280°C. For identification of the products, standard samples and Wiley library search were used.

## 3. Results and discussion

### 3.1. Electrochemical conversion results

The results of phenol concentration runs in the range 98–4698 mg $l^{-1}$ are presented along with initial solution pH values in Fig. 2 in terms of phenol removal and reaction time. Total removal of phenol was achieved in short periods of time for lower phenol concentrations, while no polymer was obtained below 482 mg $l^{-1}$. Above 2246 mg $l^{-1}$, phenol concentration, the color of the reaction medium changed from transparent to light yellow, then dark brown, and after 2 h of reaction, transparency was lost due to solid polymer particles suspended in the reactor. For 3505 mg $l^{-1}$ phenol concentration, the content of reaction medium was analyzed by HPLC and GC/MS and presented in Fig. 3 on mole percent basis with time. Due to $Cl_2$ evolved at the anode, there were only intermediate chlorinated phenol derivatives detected, in contrast to those (hydroquinone, benzoquinone, catechol, etc.) in the literature [7,8], and polymeric materials. Most likely, the rapid binding of chlorine to benzene ring led to a different reaction mechanism to prevent the formation of quinone-like compounds as reported in the literature for electrochemical oxidation products of phenol. Firstly, *p*-chlorophenol and 2,4,6-trichlorophenol formed dominantly during the electrolysis and followed by *o*-chlorophenol and then 2,4-dichlorophenol, all toxic compounds. The concentration of mono-chlorophenols started to decrease after 2 h, but

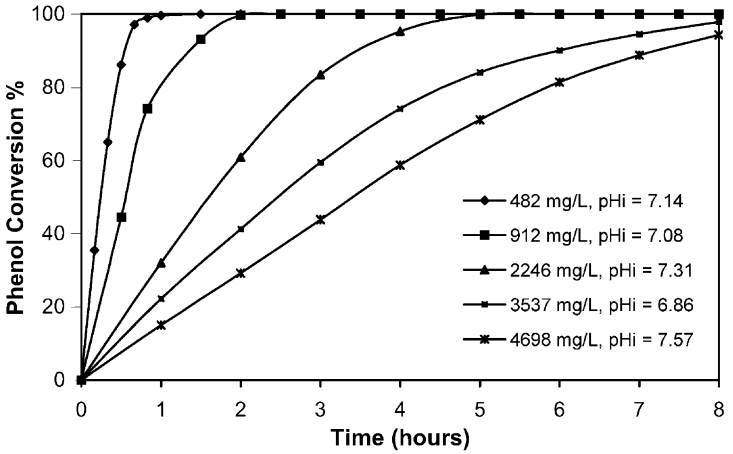


Fig. 2. The phenolic conversion (%) by reaction time for different initial phenol concentrations with initial solution pH values (current density: 32.9 mA $cm^{-2}$; NaCl concentration: 120 g $l^{-1}$; temperature: 25°C).

di- and tri-chlorophenol concentrations had their peaks around 4 h in the reaction medium. After 4 h, the concentration of polymeric compounds sharply increased suggesting the contribution of chlorophenols to polymerization. After 11 h, all intermediate products disappeared in the reaction medium, with only polymeric compounds remaining. The agitation of the medium and renewal of oxidizing agent ($Cl_2$, $ClO^-$, etc.) at the electrode probably caused most of the phenol oxidation to occur in the bulk solution, without electrode fouling, yielding non-diminishing electrode area and thus current density, unlike literature experience.

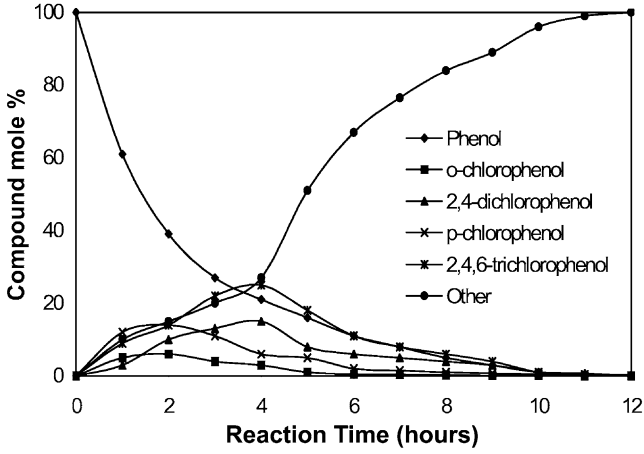


Fig. 3. The GC/MS analysis of electrochemical conversion products of phenol by reaction time (current density: 32.9 mA $cm^{-2}$; initial phenol concentration: 3505 mg $l^{-1}$; NaCl concentration: 120 g $l^{-1}$; temperature: 25°C).

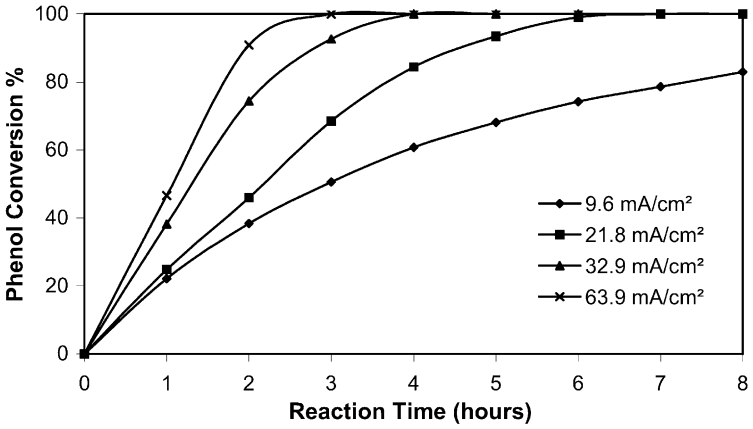


Fig. 4. The phenolic conversion (%) by reaction time for different current density values (initial phenol concentration: 3500 mg $l^{-1}$; NaCl concentration: 200 g $l^{-1}$; temperature: 25°C).

The effect of current density on removal of phenol was observed in the range 9.6–63.9 mA $cm^{-2}$ and presented in Fig. 4. In Fig. 4, the phenol removal rate increased, although not linearly, with current density, giving a sharp increase at 32.9 mA $cm^{-2}$. During the experiments up to 21.8 mA $cm^{-2}$, the transparent reaction medium changed from light yellow to dark brown while at 21.8 mA $cm^{-2}$, the light brown color was dominant throughout the run. Above 32.9 mA $cm^{-2}$ brown color of the medium turned into light green gradually and some foam formation was detected at higher initial phenol concentrations. For all runs solid polymeric materials started to form after 2 h of electrochemical oxidation.

Fig. 5 denotes the phenol removal with time voltage, respectively, at 25–45°C for 3500 mg $l^{-1}$ initial phenol concentration. In Fig. 5, after 30°C the phenol removal curves

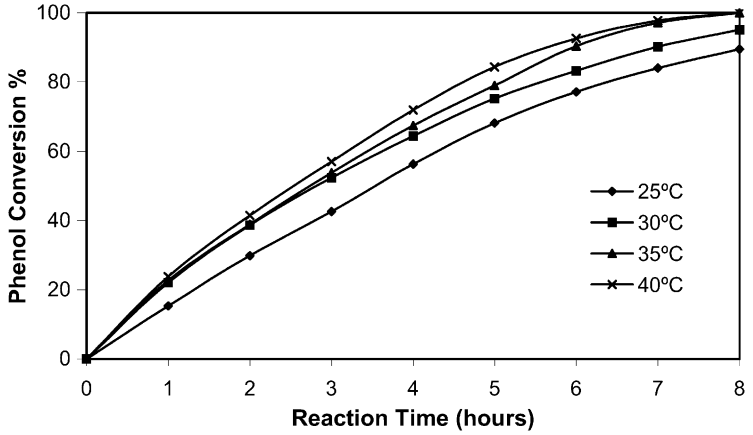


Fig. 5. The phenol conversion (%) by reaction time at different reaction temperatures (current density: 32.9 mA $cm^{-2}$; NaCl concentration: 120 g $l^{-1}$; initial phenol concentration: 3500 mg $l^{-1}$).

are almost coincident/identical, while the current density increases gradually with temperature due to increased conductivity of reaction medium. In all runs, the color of reaction medium shifted from transparent to light yellow, then to dark brown. All runs yielded solid polymeric material in decreasing quantities with temperature.

### 3.2. FTIR spectra

The FTIR spectrum of the polymer produced by electrochemical oxidation of 2246 mg $l^{-1}$ initial phenol concentration, 120 g $l^{-1}$ electrolyte (NaCl) concentration at 25°C and 32.9 mA $cm^{-2}$ current density is shown in Fig. 6.

A broad characteristic band at 3425 $cm^{-1}$ is attributed to O–H stretching modes, particularly phenolic-OH and/or OH groups attached with hydrogen bond. One would expect a sharper absorption band for OH if there were no hydrogen bond between aromatic OH groups. Therefore, one may expect repeating adjacent OH groups in the polymeric structure. The band at 3088 $cm^{-1}$ is due to aromatic C–H stretching, being a clear indication of the aromatic structure in the polymer. The band at 1501 $cm^{-1}$ is associated with an aromatic C–C stretch while the two peaks appearing at 1601 and 1647 $cm^{-1}$ may be interpreted as possible tetra-substituted groups on the aromatic ring. The sharp absorption peak at 1450 $cm^{-1}$ clearly denotes the stretching vibration of C–O bond in the aromatic ring, while the one at 861 $cm^{-1}$ is associated with out-of-plane aromatic =C–H bond deformation. The peak at 822 $cm^{-1}$ is likely due to C–Cl bond.

Other workers have also obtained FTIR spectra of polymeric films formed by electropolymerization of phenol and its derivatives. Lapuente et al. [18] employed FTIR–ATR to investigate polyphenol films formed on platinum surfaces by electrochemical oxidation of phenol in aqueous carbonate solutions with and without $Na_2S$. They obtained an intense band at 900–1150 $cm^{-1}$ associated with the ether linkages of the phenolic rings (=C–O–C=), which could not be detected in our spectra. Gattrell and Kirk [22] reported IR spectra of polyphenol produced by anodic polarization during 1 s in pH = 1 sulfuric acid solution. These authors could not detect the strong band in the 900–1150 $cm^{-1}$ associated with the ether linkages of the phenolic rings, instead a strong band at 3374 $cm^{-1}$ (O–H stretch) was seen which indicates that phenolic-OH is preserved during polymerization in contrast to the findings of Lapuente et al. [18]. However, Glarum et al. [34] again detected the same ether bands at 900–1150 $cm^{-1}$ for the polymeric films obtained by anodic polymerization for 5 min followed by treatment in chloroform and evaporation of the material onto a NaCl window. The different results indicate that the reaction conditions, as well as electrode characteristics, may change the mechanisms of the polymerization and the structure of the polymer produced.

### 3.3. STM images

Fig. 7a–e show low magnification STM images (1 μm × 1 μm scan) of polymeric films produced in electrochemical decomposition of phenol within the range 482–4698 mg $l^{-1}$ initial phenol concentration. Initial phenol concentrations lower than 482 mg $l^{-1}$ did not yield any polymeric material. Fig. 7a reveals well dispersed long polymer chains covering the whole surface of the graphite with a high chain density at 482 mg $l^{-1}$ initial phenol

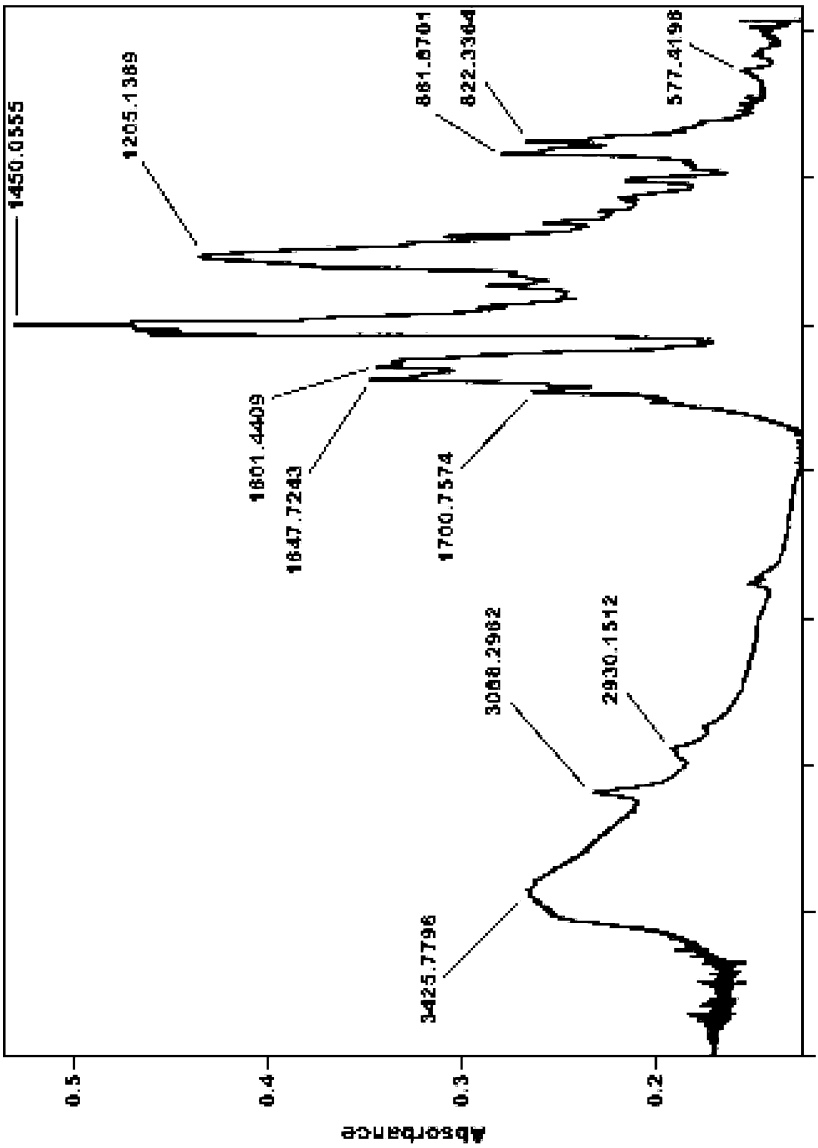


Fig. 6. The FTIR spectrum of the purified polymer sample (current density: 32.9 mA $cm^{-2}$; NaCl concentration: 120 g $l^{-1}$; initial phenol concentration: 2246 mg $l^{-1}$; temperature: 25°C).

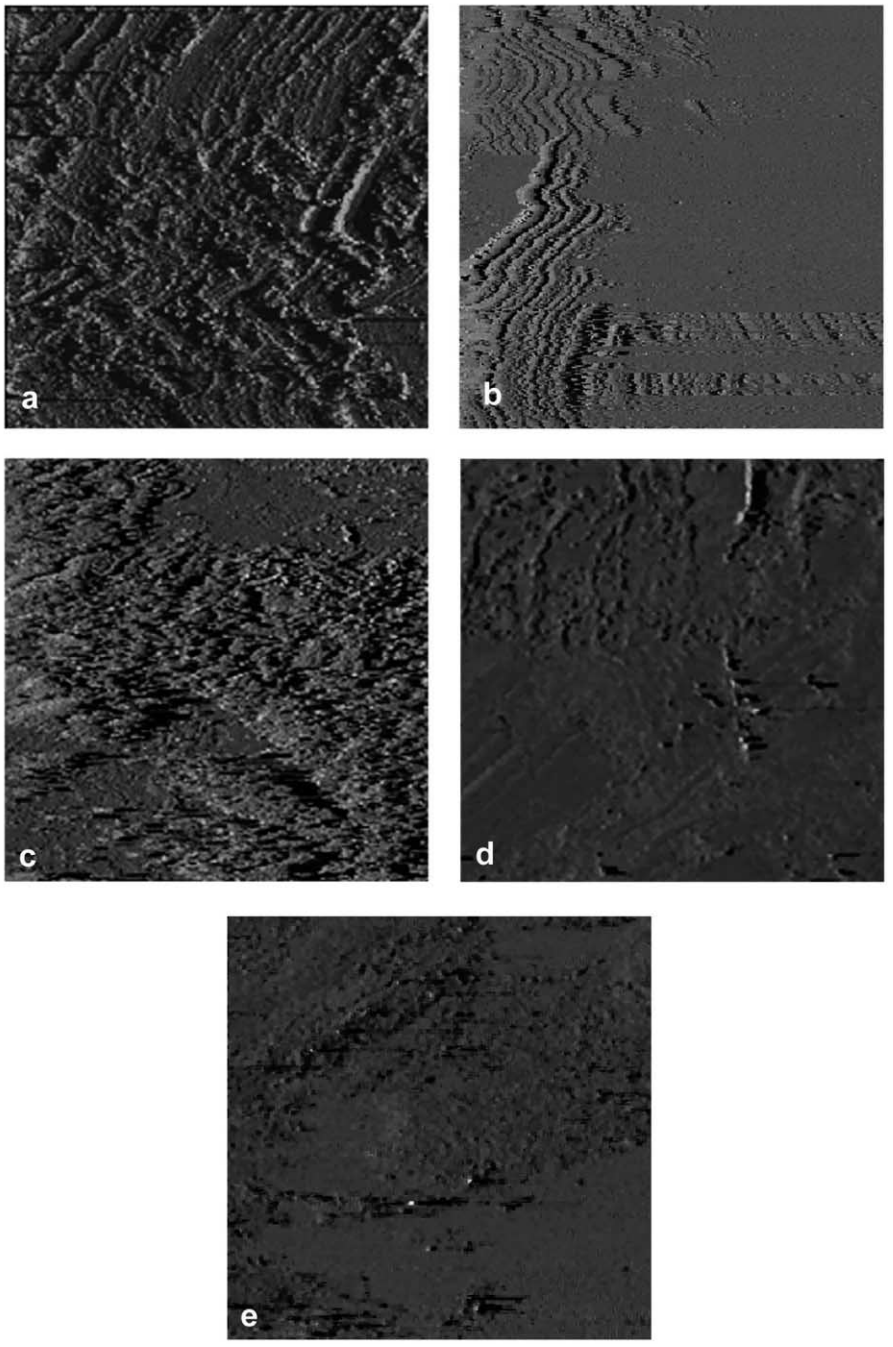


Fig. 7. The STM images (1 μm × 1 μm) of the polymer obtained for: (a) 482 mg $l^{-1}$; (b) 912 mg $l^{-1}$; (c) 2246 mg $l^{-1}$; (d) 3500 mg $l^{-1}$; (e) 4698 mg $l^{-1}$ (at current density: 32.9 mA $cm^{-2}$; NaCl concentration: 120 g $l^{-1}$; temperature: 25°C).

concentration. For Fig. 7b (912 mg $l^{-1}$) the polymer chain density diminished with respect to Fig. 7a, but the polymer chain is still longer than 1 μm, the maximum limit of STM image scale size. In Fig. 7c (2246 mg $l^{-1}$) both the density and length of the polymer chain started to decrease and the polymer was deposited on the surface in the form of aggregate. In Fig. 7d and e, for 3500 and 4698 mg $l^{-1}$ initial phenol concentrations, respectively, chain density significantly dropped and only a few short chains remained on the surface. The trend observed in the figures is consistent with that in the literature. The low level of phenol under extreme current density conditions did not yield any polymeric structure and phenol with 108 mg $l^{-1}$ initial concentration was oxidized 100% in the work of Chettiar and Watkinson [7] where $PbO_2$ anode and 316 stainless steel cathode were utilized in a $H_2SO_4$–$Na_2SO_4$ medium. But when the concentration of phenol increased, phenoxy radical concentration increased resulting in greater polymer yield. Gattrell and Kirk [8] detected the fast rate

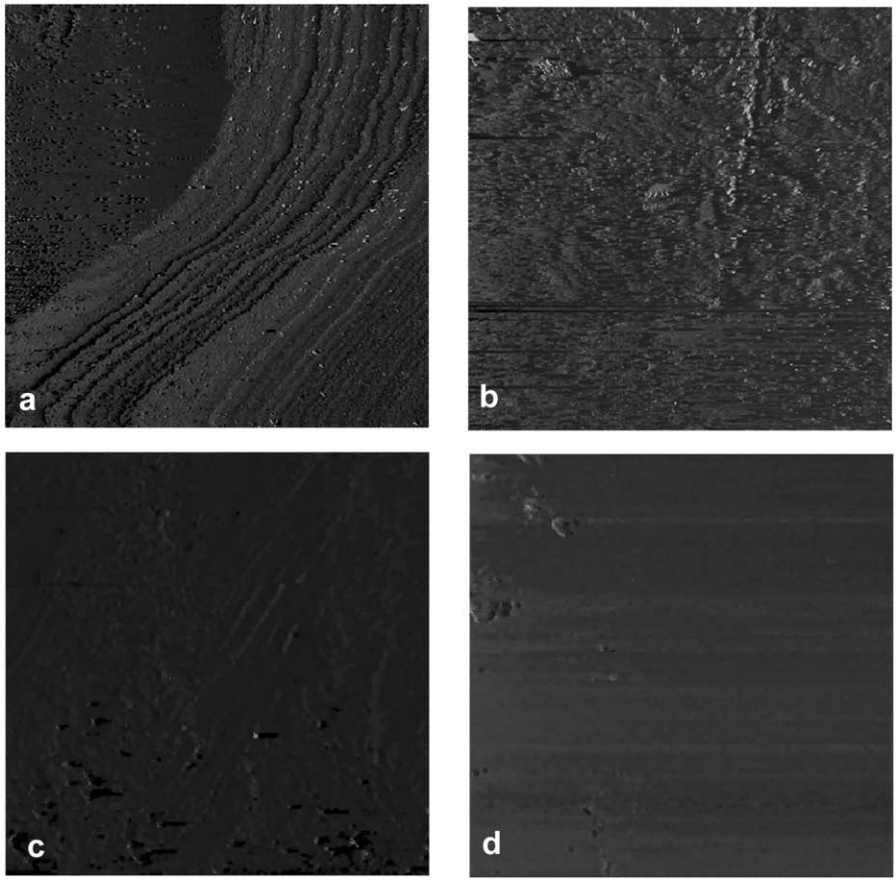


Fig. 8. The STM images (1 μm × 1 μm) of the polymer obtained for: (a) 9.6 mA $cm^{-2}$; (b) 21.8 mA $cm^{-2}$; (c) 32.9 mA $cm^{-2}$; (d) 63.9 mA $cm^{-2}$ (initial phenol concentration: 3500 mg $l^{-1}$; NaCl concentration: 200 g $l^{-1}$; temperature: 25°C).

of phenol removal and increased passivation on glassy carbon electrodes by changing the initial phenol concentration from 0 to 1920 mg $l^{-1}$ in an electrochemical cell at 1.7 V using 0.09 M sulfuric acid. However, no information has been given in the literature about the decrease of polymer molecular weight as we detected in terms of chain length decrease at high phenol concentrations.

Fig. 8a–d show the STM images (with a scan area of 1 μm × 1 μm) obtained at constant 3500 mg $l^{-1}$ initial phenol concentration for current density range 9.6–63.9 mA $cm^{-2}$. Fig. 8a (for 9.6 mA $cm^{-2}$) depicts clearly visible polymer chains longer than 1 μm placed diagonally and right down on the graphite surface while upper left region does not contain any polymer. Small circular stains scattered over the image are attributed to impurities. Fig. 8b (21.8 mA $cm^{-2}$) contained short dense polymer chain, but the density drops in Fig. 8c (32.9 mA $cm^{-2}$) and becomes almost zero in Fig. 8d (63.9 mA $cm^{-2}$). As observed in the work of Gattrell and Kirk [8], high anodic voltage with increased current density oxidized the phenoxy radicals, decreasing its concentration and polymer formation while oxidation of phenol into intermediate and final products were favored. On the other hand, at lower potentials, almost all of the phenol removed could be accounted for as polymeric products.

Fig. 9a and b shows the STM images (with a scan area of 1 μm × 1 μm) of the polymer produced at 25 and 30°C, respectively, for 32.9 mA $cm^{-2}$ and 3500 mg $l^{-1}$ initial phenol concentration. Higher temperatures did not yield significant STM images, and not presented. Fig. 9a has short polymer chains with high density while Fig. 9b shows again small polymer chains with low density on the surface. This result is in accord with the literature where high oxidation temperatures seemed to reduce or prevent the passivation of the electrode with phenolic polymers [8].

Fig. 10 shows a magnified region from Fig. 7b with a scan area of 20 nm × 20 nm. The repeating units in the polymer backbone (with a width of 2.92 nm) belong to phenols with side groups irregularly attached to the ring chain.

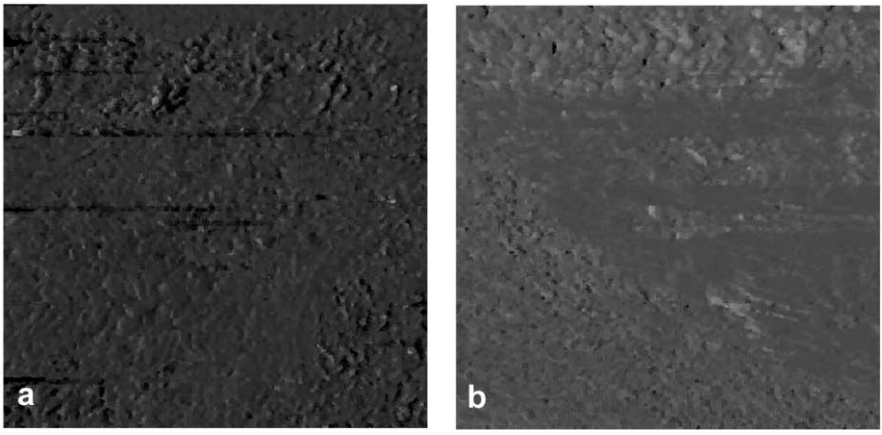


Fig. 9. The STM images (1 μm × 1 μm) of the polymer obtained for: (a) 25°C; (b) 30°C (at current density: 32.9 mA $cm^{-2}$; NaCl concentration: 120 g $l^{-1}$; initial phenol concentration: 3500 mg $l^{-1}$).

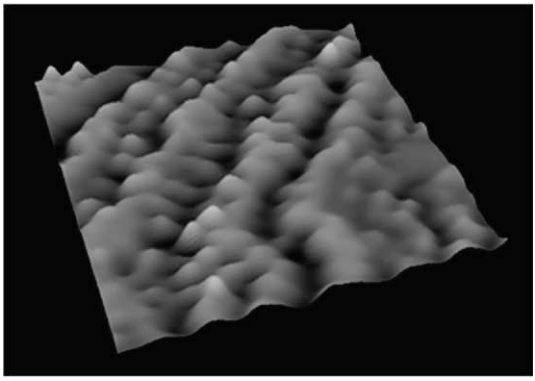

Fig. 10. A magnified STM vision (20 nm × 20 nm) of a region in Fig. 7b (at current density: 32.9 mA $cm^{-2}$; NaCl concentration: 120 g $l^{-1}$; temperature: 25°C; initial phenol concentration: 912 mg $l^{-1}$).

Richard and Gewirth [24] has made use of STM to monitor the electrooxidation of phenoxide to oligophenol on Au(1 1 1) in alkaline solutions. They observed amorphous, disordered structures, which interfered with imaging obtained at +50 mV in a solution containing $1 \times 10^{-4}$ M phenol and 0.1 M $NaClO_4$ with KOH added to give a pH value of 9.3 [24]. Wang and Martinez [25] used STM to investigate the formation of inhibitory polyphenol layers on glassy carbon surfaces. Their STM images were obtained after electrodeposition from 1.0 mM solutions of the phenols, by sweeping the potential between 0 and 1.3 V at different rates for a set number of cycles, or by holding the potential constant in this range. They found that microstructures of the phenolic films produced on the electrode were markedly dependent on the anodization conditions, but they could not correlate molecular structure of the polymer with these conditions due to low resolution of their images and lack of FTIR or other analytic tools. In our work, we examined the formation of non-passivating polymeric products as a function of electrochemical conversion conditions by means of STM images and FTIR and correlated the results with other works in the literature.

## 4. Conclusions

In this work, we have accomplished the first non-passivating polymer formation in the presence of NaCl during electrochemical conversion of phenol using carbon electrodes. There has been no work in literature stating the polymer production and non-passivating polymer formation under the similar set-up and process parameters we employed. STM images and FTIR analysis were used to visualize the influence of initial phenol concentration, current density and reaction temperature on polymer morphology and structure, respectively. Solid polymer was produced at high voltage and current density values compared to the literature, with most orderly form at 912 mg $l^{-1}$ initial phenol concentration, current density 32.9 mA $cm^{-2}$, NaCl concentration 120 g $l^{-1}$ and temperature 25°C. Higher operational parameters yielded STM images of polymer aggregates in decreasing surface density. During electrochemical conversion, only toxic mono-, di- and tri-chlorophenols were formed

as intermediate compounds just like in chemical oxidation with sodium hypochloride, but eventually they were polymerized and/or oxidized to final products. FTIR analysis and the enlarged STM image implied the repeating phenol units and chlorine in the polymer structure. Our results may inspire an alternative treatment of phenolic wastewaters by converting phenol into the form of a solid polymer.

## Acknowledgements

This project was supported by Hacettepe University Research Fund with Project no.: 98.02.602.004.

## References

[1] K.H. Lanouette, Chem. Eng. 84 (1977) 99.
[2] Y.M. Awad, N.S. Abuzaid, J. Environ. Sci. Health A32 (1997) 1393.
[3] Ch. Comninellis, C. Pulgarin, J. Appl. Electrochem. 23 (1993) 108.
[4] A.B. Boscoletto, F. Gottardi, L. Milan, P. Pannocchia, V. Tartari, R. Amadelli, A. de Battisti, A. Barbieri, D. Patracchini, G. Battaglin, J. Appl. Electrochem. 24 (1994) 1052.
[5] Ch. Comninellis, A. Nerini, J. Appl. Electrochem. 25 (1995) 23.
[6] M. Gattrell, D.W. Kirk, J. Electrochem. Soc. 140 (1993) 903.
[7] M. Chettiar, A.P. Watkinson, Can. J. Chem. Eng. 61 (1983) 568.
[8] M. Gattrell, D.W. Kirk, Can. J. Chem. Eng. 68 (1990) 997.
[9] A. Dabrowski, J. Mieluch, A. Sadkaoski, J. Wild, P. Zoltowski, Prezm. Chem. 54 (1975) 653.
[10] J.D. Santlebury, V. Ashwoth, B. Yap, J. Oil Colour Chem. Assoc. 61 (1978) 335.
[11] G. Mengoli, P. Bianco, S. Daolio, M.T. Munari, J. Electrochem. Soc. 128 (1981) 2276.
[12] G. Mengoli, S. Daolio, M.M. Musiani, J. Appl. Electrochem. 10 (1980) 459.
[13] J. Wang, M.S. Lin, Anal. Chem. 60 (1988) 499.
[14] R.C. Koile, D.C. Johnson, Anal. Chem. 51 (1979) 741.
[15] M. Poon, R.L. McCreery, Anal. Chem. 58 (1986) 2745.
[16] L. Papouchado, R.W. Sandford, G. Petrie, R.N. Adams, J. Electroanal. Chem. 65 (1975) 275.
[17] Z. Zwierzehowska-Nowakowska, M. Bosak, Biul. Wojsk. Akak. Tech. 31 (1982) 63.
[18] R. Lapuente, F. Cases, P. Garce's, E. Morallo'n, J.L. Va'zques, J. Electroanal. Chem. 451 (1998) 163.
[19] F. Bruno, M.C. Phan, J.E. Dubois, Electrochim. Acta 22 (1977) 451.
[20] P. Mourcell, M.C. Phan, P.C. Lacaze, J.E. Dubois, J. Electroanal. Chem. 145 (1983) 467.
[21] M. Delamar, M. Chemini, J.E. Dubois, J. Electroanal. Chem. 169 (1984) 145.
[22] M. Gattrell, D.W. Kirk, J. Electrochem. Soc. 139 (1992) 2738.
[23] M. Fleischmann, I.R. Hill, G. Mengoli, M.M. Musiani, Electrochim. Acta 28 (1983) 1545.
[24] K.M. Richard, A.A. Gewirth, J. Phys. Chem. 99 (1995) 12288.
[25] J. Wang, T. Martinez, D.R. Yaniv, L.D. McCormick, J. Electroanal. Chem. 313 (1991) 129.
[26] G. Binning, H. Rohrer, Helv. Phys. Acta 55 (1982) 726.
[27] R. Yang, X.R. Yang, D.F. Evans, W.A. Hendrickson, J. Baker, J. Phys. Chem. 94 (1990) 6123.
[28] Z.Q. Xue, H.J. Gao, W.M. Liu, C. Zhu, Z. Ma, S. Pang, Appl. Surf. Sci. 61 (1992) 346.
[29] L.M. Eng, H. Fuchs, K.D. Jandt, J. Petermann, in: Proceedings of the Conference of American Institute of Physics, 1991, pp. 241–262.
[30] W.G. Morris, D.M. White, J.L. Gordon, T. Thund, J. Vac. Sci. Technol. A 10 (1992) 623.
[31] C. Koçum, M.H. Zareie, F. Özer, E. Piskin, Coll. Polym. Sci. 278 (2000) 587.
[32] R. Ikeda, J. Sugihara, H. Uyama, S. Kobayashi, Macromolecules 29 (1996) 8702.
[33] M.H. Zareie, PhD Dissertation, Scanning Tunneling Microscope: Design, Construction and Applications, Hacettepe University, Ankara, Turkey, 1995.
[34] S.H. Glarum, J.H. Marshall, M.Y. Hellman, G.N. Taylor, J. Electrochem. Soc. 134 (1987) 81.